SOLUBILITY LIMITS OF ERBIUM IN PARTIALLY DISORDERED CRYSTALS LANGANITE AND LANGATATE*

O. TOMA, L. GHEORGHE, R. BIRJEGA

National Institute for Laser, Plasma and Radiation Physics, 409 Atomistilor Street, Magurele, Jud. Ilfov, 077125, Romania, E-mail: octavian.toma@inflpr.ro

Received September 5, 2011

Solubility limits of Er^{3+} in partially disordered crystalline compounds langanite ($La_3Ga_{5.5}Nb_{0.5}O_{14}$) and langatate ($La_3Ga_{5.5}Ta_{0.5}O_{14}$) are reported. The compounds are synthesized by solid-state reaction. X-ray powder diffraction analysis is used to determine the solubility limit of Er^{3+} in the two compounds.

Key words: Partially disordered crystals, erbium, LGN, LGT.

1. INTRODUCTION

The development of new efficient photovoltaic cells for solar energy conversion is an important challenge nowadays. One of the approaches of this problem is to increase the efficiency of silicon photovoltaic cells by conversion of the solar radiation emitted around 1.5 μm in radiation situated in the spectral range around 1 μm, that can be converted efficiently in electric energy [1]. This spectral conversion can be made by upconversion processes in Er^{3+} ions, which have an intense absorption band around 1.5 μm (transition $^4I_{15/2} \rightarrow {}^4I_{13/2}$) and can emit efficiently around 1 μm (transition $^4I_{11/2} \rightarrow {}^4I_{15/2}$). The efficiency of Er^{3+} for this task can be enhanced by the broadening of its absorption bands; this will cause an increase of the absorbed solar energy emitted in the large band around 1.5 μm and may also cause an increase of the rates of upconversion processes that accomplish the spectral conversion. For the broadening of the absorption spectra of Er^{3+}, partially disordered crystals can be used as its hosts. Langanite ($La_3Ga_{5.5}Nb_{0.5}O_{14}$ – LGN) and langatate ($La_3Ga_{5.5}Ta_{0.5}O_{14}$ – LGT) are such crystals.

* Paper presented at the 12th International Balkan Workshop on Applied Physics, July 6–8, 2011, Constanta, Romania.

LGN and LGT crystallize in the *P321* space group, symmetry class *32* and are isostructural with the calciumgallogermanate ($Ca_3Ga_2Ge_4O_{14}$) [2]. Their general formula is $A_3BC_3D_2O_{14}$ where *A* represents the dodecahedral positions (distorted Thompson cubes), *B* – octahedral positions and *C*, *D* – tetrahedral positions. La^{3+} occupies the position *A*. The local symmetry at this site is C_2 [3]. The disorder of these crystals is given by the occupation of the octahedral positions *B*, with equal probability, by two different ions. In LGN the octahedral positions *B* are occupied by Ga^{3+} and Nb^{5+}, while in LGT these positions are shared by Ga^{3+} and Ta^{5+}. Ga^{3+} occupies the remaining positions (*C* and *D*).

Although there are a few studies [4,5] regarding the luminescence properties of erbium-doped LGN and LGT, there is no information in the scientific literature about the solubility limits of erbium in these compounds.

In this paper, we investigate, for the first time to our knowledge, the solubility limits of erbium in LGN and LGT using X-ray diffraction analysis.

2. EXPERIMENTAL

LGN and LGT samples doped with various erbium concentrations were prepared using a solid-state reaction route. The raw materials used for LGN were: La_2O_3 (Alfa Aesar, 99.999%), Ga_2O_3 (Alfa Aesar, 99.999%), Nb_2O_5 (Johnson Matthey Chemicals Ltd., Spectrographically Standardised), and Er_2O_3 (Aldrich Chem. Co., 99.99+%). For the synthesis of LGT, Ta_2O_5 (Alfa Aesar, 99.993%) was used instead of Nb_2O_5. For each sample, the raw materials were mixed in the right proportion and homogenized using an agate mortar and pestle; the mixture was then pressed in a pellet and thermally treated at 1350ºC for 36 h in a Nabertherm LHT 02/18 furnace. Polycrystalline ceramic pellets were obtained. The pellets were afterwards ground in the agate mortar for the powder X-ray diffraction analysis.

For the X-ray diffraction analysis, a PANalytical 'XPert PRO MPD diffractometer was used counting 2 s per 0.02º 2θ for the whole pattern and 20 s per 0.02º 2θ for the restricted 29.5º - 34º angular domain. In the diffracted beam, a Ni filter, a curved graphite monochromator and a programmable divergence slit, enabling constant sampling area irradiation, were placed ($\lambda = 0.15418$ nm).

3. RESULTS AND DISCUSSION

As the difference between the ionic radii of Er^{3+} (1.004 Å) and La^{3+} (1.16 Å) in dodecahedral coordination [6] is relatively high, distortions of the crystalline cell are expected when a great number of La^{3+} ions are substituted by Er^{3+}. Therefore,

we expected a low solubility limit of Er^{3+} in both compounds. The investigation was started with LGN and LGT samples doped with 20 at. % Er^{3+}; as the X-ray diffraction patterns of both samples presented supplementary diffraction peaks characteristic to other crystalline phases, the erbium concentration was decreased progressively until reaching the solubility limit at erbium concentrations where the diffraction patterns no longer present peaks specific to parasite crystalline phases.

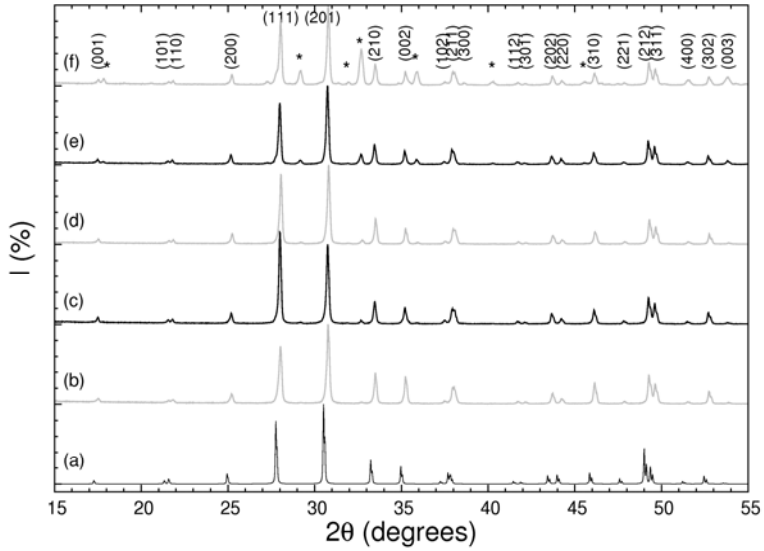

Fig. 1 – X-ray diffraction patterns obtained for Er:LGN samples with various erbium concentrations: (a) - XRD simulated pattern of the LGN standard (JCPDS file no. 047-0533); (b) - Er(3 at. %):LGN; (c) - Er(4 at. %):LGN; (d) - Er(5 at. %):LGN; (e) - Er(10 at. %):LGN; (f) - Er(20 at. %):LGN. The lines of the dominant LGN phase were labeled with Miller indices; label * designates the $Er_3Ga_5O_{12}$ parasite phase.

The X-ray diffraction patterns obtained for the Er:LGN and Er:LGT samples are presented in Figs. 1 and 2, respectively; the lines of the LGN (JCPDS file no.047-0533 [7]) and LGT (JCPDS file no. 047-0532 [7]) phases were labeled with the corresponding Miller indices, while the lines of parasite crystalline phases were labeled with an asterisk. All patterns are normalized at the maximum intensity and shifted vertically for a better view. The XRD patterns of the dominant langanite / langatate phases are slightly shifted towards higher angles in comparison with their corresponding standards indicative of smaller lattice parameters values which are consistent with the replacement of the lanthanum ions (of larger ionic radius) by erbium (having a smaller ionic radius) [6].

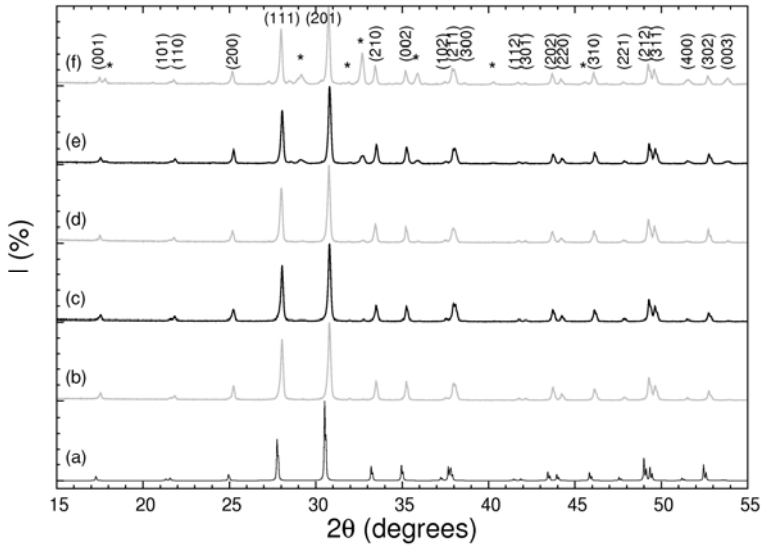

Fig. 2 – X-ray diffraction patterns obtained for Er:LGT samples with various erbium concentrations: (a) - the XRD simulated pattern of the LGT standard (JCPDS file no. 047-0532); (b) - Er(3 at. %):LGT; (c) - Er(4 at. %):LGT; (d) - Er(5 at. %):LGT; (e) - Er(10 at. %):LGT; (f) - Er(20 at. %):LGT. The lines of the dominant LGT phase were labeled with Miller indices; label * designates the $Er_3Ga_5O_{12}$ parasite phase.

Table 1

The Miller indices corresponding to the lines of $Er_3Ga_5O_{12}$ observed in the X-ray diffraction patterns of Er:LGN/LGT

2θ (°)	Miller indices
17.81-17.83	2 1 1
29.15-29.16	4 0 0
32.66-32.67	4 2 0
35.86-35.87	4 2 2
40.29	5 2 1
45.55-45.59	6 1 1

In Figs. 1 and 2 parasite lines can be found at 2θ = 17.81-17.83°, 29.15-29.16°, 32.66-32.67°, 35.86-35.87°, 40.29°, and 45.55°-45.59°. All these lines could be identified with lines of the garnet $Er_3Ga_5O_{12}$ (JCPDS no. 012-0769) [7] (their Miller indices are specified in Table 1). This garnet phase includes the erbium excess in samples with concentrations above the solubility limit.

In order to scrutinize the evolution of the $Er_3Ga_5O_{12}$ parasitic phase relative to the erbium concentration, the XRD patterns in 2θ = 29.5º - 34º range were collected using a higher acquisition time on each step. The corresponding XRD patterns of this particular domain containing the peaks of the highest intensities of both the main LGN/LGT phases and of the parasitic garnet phase (201) and (420),

respectively, are presented in Figs. 3 and 4, normalized at the intensity of the (201) reflection of the LGN/LGT phase. There are no LGN/LGT reflections overlapping the (420) line of the garnet $Er_3Ga_5O_{12}$; therefore, the relative intensity of the (420) parasitic $Er_3Ga_5O_{12}$ line will be an indicator of the solubility of Er in the host crystals (Fig. 5). Figs. 3 - 5 reveal the expected increase of this relative intensity with the increase of the erbium concentration. In addition, for the highest Er concentrations extra-peaks of very low intensities could be observed. They are assignable to impurity phases $LaGaO_3$ (JCPDS 70-2784 [7]) and β-Ga_2O_3 (JCPDS 41-1103 [7]).

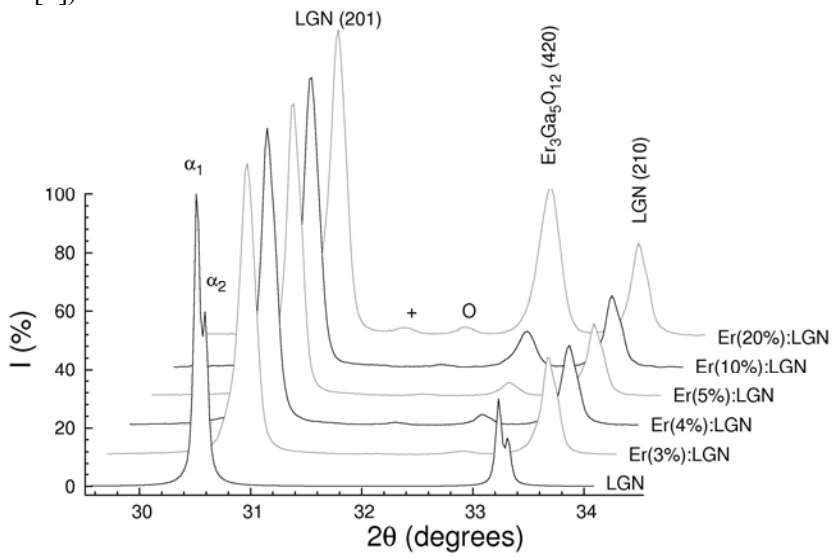

Fig. 3 – The XRD patterns of Er:LGN series of samples in the $2\theta = 29.5^\circ$ - 35° region. O stands for the overlapped (121) and (200) peaks of a $LaGaO_3$ impurity phase and + stands for the (-202) peak of a β-Ga_2O_3 impurity phase. The pattern labeled LGN represents the XRD simulated pattern of the LGN standard (JCPDS file no. 047-0533), and α_1 and α_2 denote the reflections corresponding to Cu Kα1, respectively Kα2 radiation.

As Figs. 3–5 depict, the values of the relative intensity of the garnet (420) reflection in LGN are systematically higher than the corresponding values of the relative intensity of the same line in LGT. This denotes a lower solubility limit of Er in LGN in comparison with the LGT, although the crystallographic parameters of the two host crystals (unit cell volume, average La-O distances) are almost identical [8]. Indeed, at 3 at. % Er concentration for LGT no parasitic peak of $Er_3Ga_5O_{12}$ phase could be observed while for 4 at. % Er concentration an extremely ill-defined peak could be perceived, similar to the one observed in the Er(3 at. %):LGN XRD pattern. Therefore, the values of the solubility limit of Er in LGN and LGT were approximated to 3 at. %, respectively 4 at. %.

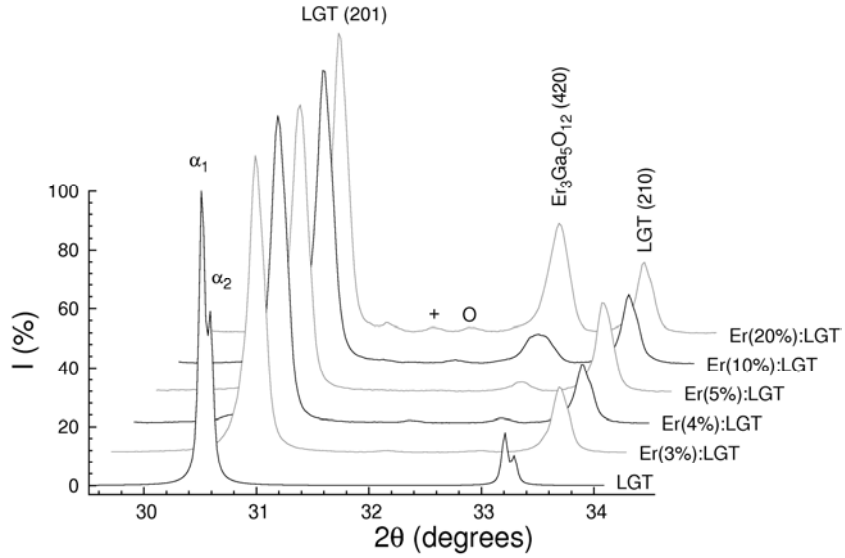

Fig. 4 – The XRD patterns of Er:LGT series of samples in the $2\theta = 29.5^{\circ}$ - 35° region. O stands for the overlapped (121) and (200) peaks of a $LaGaO_3$ impurity phase and + stands for the (-202) peak of a β-Ga_2O_3 impurity phase. The pattern labeled LGT represents the XRD simulated pattern of the LGT standard (JCPDS file no. 047-0532), and α_1 and α_2 denote the reflections corresponding to Cu Kα1, respectively Cu Kα2 radiation.

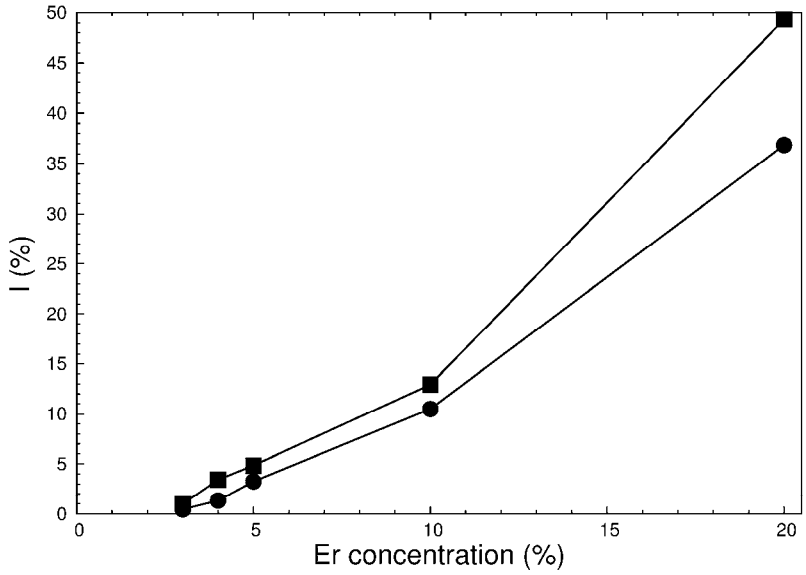

Fig. 5 – The evolution of the relative intensity of the (420) reflection of the $Er_3Ga_5O_{15}$ parasitic phase as a function of Er concentration in LGN (full squares) and LGT (full circles).

4. CONCLUSIONS

Langanite and langatate powder samples doped with erbium ions in various concentrations were synthesized by solid-state reaction. The structure of the samples was investigated by X-ray powder diffraction. The solubility limits of erbium in the investigated crystals were estimated as 3 at. % in langanite and 4 at. % in langatate.

Acknowledgements. This work was supported by the post doctoral research project no. 159/13.08.2010 of the Romanian National Council of Scientific Research (CNCS).

REFERENCES

1. B. S. Richards, *Enhancing the performance of silicon solar cells via the application of passive luminescence conversion layers*, Solar Energy Materials & Solar Cells **90**, 2329–2337 (2006).
2. B. V. Mill, A. V. Butashin, G. G. Kodzhabagian, E. L. Belokoneva, N. V. Belov, Doklady Akademii Nauk SSSR **264**, 1385 (1982).
3. N. Molchanov, B. A. Maksimov, A. F. Kondakov, T. S. Chernaya, Yu. V. Pisarevsky, V. I. Simonov, JETP Lett. 74, 222 (2001).
4. F. P. Yu, D. R. Yuan, S. Y. Guo, X. L. Duan, X. Q. Wang, L. M. Kong, X. Q. Zhang, X. Zhao, *Effects of Er^{3+} doping concentration and calcination on fluorescence properties of $La_3Ga_{5.5}Nb_{0.5}O_{14}$ nanocrystals*, Crystal Research and Technology **43**, 522–525 (2008).
5. W. Ryba-Romanowski, G. Dominiak-Dzik, P. Solarz, M. Berkowski, *Optical study of erbium-doped $La_3Ga_{5.5}Ta_{0.5}O_{14}$ single crystal*, Molecular Physics **101**, 1067–1072 (2003).
6. R. D. Shannon, *Revised Effective Ionic Radii and Systematic Studies of Interatomic Distances in Halides and Chalcogenides*, Acta Crystallographica **A32**, 751–767 (1976).
7. JCPDS files, International Center for Diffraction Data (ICDD), Newton Square, PA. USA, (2010).
8. A. P. Dudka, B. V. Mill, Yu. V. Pisarevsky, *Refinement of the crystal structures of the $La_3Ta_{0.5}Ga_{5.5}O_{14}$ and $La_3Nb_{0.5}Ga_{5.5}O_{14}$ Compounds*, Crystallography Reports **54**, 558–567 (2009).